Fall 2020

# Diagonalization of 1-D Schrodinger Operators with Piecewise Constant Potentials

Sarah Wright

# DIAGONALIZATION OF 1-D SCHRÖDINGER OPERATORS WITH PIECEWISE CONSTANT POTENTIALS

by

Sarah Daley Wright

A Thesis
Submitted to the Graduate School,
the College of Arts and Sciences
and the School of Mathematics and Natural Sciences
of The University of Southern Mississippi
in Partial Fulfillment of the Requirements
for the Degree of Master of Science

December 2020

ABSTRACT

In today's world our lives are very layered. My research is meant to adapt current inefficient numerical methods to more accurately model the complex situations we encounter. This project focuses on a specific equation that is used to model sound speed in the ocean. As depth increases, the sound speed changes. This means the variable related to the sound speed is not constant. We will modify this variable so that it is piecewise constant. The specific operator in this equation also makes current time-stepping methods not practical. The method used here will apply an eigenfunction expansion technique used in previous research that eliminates the current time-stepping problems.

Key words: Partial differential equations, Schrödinger operator, The Secant Method, Matrix Determinant Lemma

# ACKNOWLEDGMENTS

I would like to express my sincere gratitude to my advisor, Dr. James Lambers, for his continuous support of my Master's Thesis, for his patience, and motivation. His enthusiasm for teaching and seeing students learn has inspired me in so many ways. Thank you to my committee members Dr. Tian and Dr. Zhu for your time and feedback. I would also like to thank my family and friends who have been a source of endless encouragement throughout this process.

# TABLE OF CONTENTS

# LIST OF ILLUSTRATIONS

**Figure**

# LIST OF TABLES

**Table**

# LIST OF ABBREVIATIONS

**PDE** - Partial Differential Equation
**ODE** - Ordinary Differential Equation

# Chapter 1

# BACKGROUND

## 1.1 Introduction

This research is primarily focused on applications of numerical analysis in order to model real world problems that have many layers. The world we live in has many layers and our simulation methods need to account for this. Specifically, we want to be able to more accurately and quickly simulate time-dependent physical phenomena such as heat diffusion, wave propagation, or fluid flow through heterogeneous media. Equations that are used to model these type of problems are called partial differential equations (PDEs). A very well known PDE is the wave equation

$$u_{tt} = \alpha^2 u_{xx}$$

where

$$\begin{aligned} u_{tt} &= \text{the second derivative of the solution with respect to time} \\ \alpha &= \text{wave speed} \\ u_{xx} &= \text{concavity of the solution curve [5].} \end{aligned}$$

This PDE can be used to model any energy that travels in waves. This could be seismic energy, a vibrating string, pressure from a liquid, or displacement of a gas over a certain length of time. The unknown solution $u(x,t)$ is a function of two variables and this equation contains its derivatives with respect to individual variables. When graphed, this solution, $u(x,t)$, looks like a wave for Figure 1.1.

This equation can be solved using conventional analytical methods such as separation of variables because the coefficient $\alpha^2$ is constant. We assume the equation is being used to model the vertical displacement of a string from the $x$ axis with position $x$ at time $t$. The string has length $l$ and Dirichlet boundary conditions meaning

$$u(0,t) = 0, \quad t > 0 \tag{1.1}$$

$$u(l,t) = 0, \quad t > 0. \tag{1.2}$$

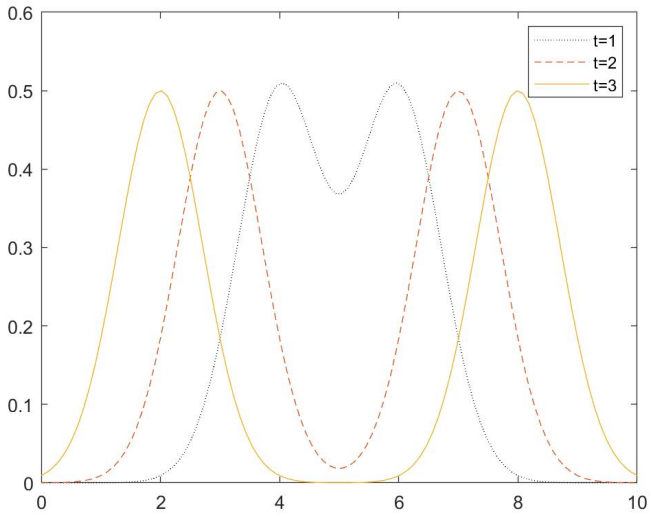


*Figure 1.1*: This figure shows the solution of $u(x,t)$ to the wave equation with initial conditions $u(x,0) = e^{-(x-5)^2}$ and $u_t(x,0) = 0$ at times $t = 1$, $t = 2$, and $t = 3$.

with initial conditions

$$u(x,0) = f(x), \quad 0 < x < l \tag{1.3}$$

$$u_t(x,0) = g(x), \quad 0 < x < l \tag{1.4}$$

for some known functions $f(x)$ and $g(x)$. We are being asked to solve for $u(x,t)$ for all $x$ and $t$.

First we want to find a solution that is a combination of functions that depend on only one variable such that

$$u(x,t) = X(x)T(t).$$

Now we will substitute this into our PDE to obtain

$$X(x)T''(t) = \alpha^2 X''(x)T(t).$$

This can be rewritten as

$$\frac{X''(x)}{X(x)} = \frac{T''(t)}{\alpha^2 T(t)}.$$

Now the left hand side is not dependent on $t$ and the right hand side is not dependent on $x$. Both sides must be equal for all values of $x$ and $t$; therefore, we can set each side equal to a constant, $-\lambda$.

$$\frac{X''(x)}{X(x)} = -\lambda \tag{1.5}$$

$$\frac{T''(t)}{\alpha^2 T(t)} = -\lambda \tag{1.6}$$

These equations can be used to obtain the Ordinary Differential Equations (ODEs)

$$X''(x) + \lambda X(x) = 0 \tag{1.7}$$

$$T''(t) + \alpha^2 \lambda T(t) = 0. \tag{1.8}$$

The equation for $X$ is actually an eigenvalue problem where $X$ is the eigenfunction and $\lambda$ is the eigenvalue. Solving these ODEs is trivial because eigenfunctions can be found for $X$ and $T$ in order to form the solution $u(x,t)$. However, the PDE we are working with does not have a constant coefficient. The coefficient we will be working with is piecewise constant. This means that the solution wave will travel at a certain frequency depending on the medium it is traveling through. Similar to the conventional method of separation of variables that leads to an eigenfunction expansion, we will attempt a similar method using eigenfunction expansions; however, the eigenfunctions must be computed differently due to the piecewise constant coefficient [1]. In previous research, we have used the Uncertainty Principle and numerical methods in order to find the natural frequencies where the discontinuities occur. We hypothesise that similar methods can be applied to a different PDE with piecewise constant coefficients.

Our algorithm's approach will be to find these natural frequencies that will simplify the problem. Another factor that is important to this research is being able to use today's technology at its highest capacity by using simulation methods at high resolutions. However, using current simulation methods, as you increase the resolution, the time step length shrinks so that the number of time steps needed grows exorbitantly, which causes the method to lose efficiency. This is largely because conventional analytical methods are not "scalable". [8] We hypothesize that we will be able to develop a scalable numerical method that will solve PDEs with non-constant coefficients.

The problem that this research will be looking at is a PDE that is used to model acoustic pressure in the ocean. This specific equation is called the parabolic equation and it is a factor of the Helmholtz equation. The Helmholtz equation is an eigenvalue problem for the Laplacian operator and has many applications in physics. We will be using an eigenvalue problem to help solve the parabolic equation and one of the applications of our research will be to develop a better algorithm for solving the Helmholtz equation [9].

The Helmholtz equation, also known as the two-way wave equation, can be factored to represent the forward and backward movement of waves. We will isolate the equation representing forward propagation and refer to it as the "one way equation". The coefficient in this equation is non constant because it is used to represent sound speed at different depths

of the ocean. This equation only models waves traveling in one direction and so we must assume that any motion in the opposite direction, such as echoes, are negligible. Labs such as NRL have acquired data that shows that this coefficient, although it is not constant, is nearly piecewise constant. We will look at the three piece case, where the first and last piece are taken from the true sound speed and the middle piece is almost constant. From the data collected at the lab, we can take an average of the sound speed on an interval and use that as the second piece coefficient.

An interesting aspect of this "one-way equation" is that it includes a scalar multiple of a Schrödinger operator. A typical Schrödinger operator is the sum of the kinetic energies, which will involve a constant times the Laplacian operator, and the potential energies [14]. The Schrödinger operator is important in mathematical physics and plays a role in many wave equations. Our operator in the "one-way" equation is a scalar transformation of the Schrödinger operator because our coefficient of the Laplacian is one [6].

Although this research is connected to previous research done with eigenvalue problems, there are many differences which make it more difficult and have more practical applications to simulate layered situations. In previous work, all of the eigenvalues are positive and lead to a uniform method of solving for all eigenvalues; however, in this project, we will see that both negative and non-negative eigenvalues are involved which will affect how we choose to construct the eigenfunction. Another problem that arises in this project occurs when you take the square root of the operator. Under usual circumstances like in previous research, you would use a numerical method to discretize the operator by a matrix, apply a time stepping method, and solve the resulting system of equations if using an implicit time-stepping method; however, this cannot be done in this case. Taking the square root of the operator makes implementing a time-stepping method more difficult. It has been shown that the square root of an operator can be approximated by using the “rational approximation" of $\sqrt{Q}$ where $Q$ is the operator obtained by

$$\alpha_0\sqrt{1+q}$$

where

$$q=\frac{Q}{\alpha_0^2}-1.$$

In order to obtain an accurate approximation, this square root needs to be expanded using Taylor expansion by setting

$$\sqrt{1+q}=1+\frac{q}{2}.$$

Using Taylor expansion is computationally expensive and in order to achieve higher accuracy, you need many terms. The method of finding the rational approximation for the operator

will require a different approach.

## 1.2 Outline

In this chapter I have introduced the research area, the need for this scalable numerical method in the face of our very layered world, and the specific PDE that I will be working with. In Chapter 2, I will discuss the background of this equation in more detail mathematically. I will address the mathematical dillemas that were presented in working with this problem, the existing approaches that motivate the development of a more efficient algorithm, and my previous research that contributed to this numerical method. In Chapter 3, I will include the detailed methodolgy and approach to this research topic. Chapter 4 will be a compilation of all of the numerical results obtained using the algorithm. This will include efficiency and analysis and comparison of my results to those of existing approaches. Finally, Chapter 5 will conclude this thesis with final thoughts regarding the method and possible future work that could use similar approaches.

# Chapter 2

# Background

The equation discussed previously that models acoustic pressure in the ocean is the Helmholtz equation

$$\left(\frac{\partial^2}{\partial r^2}+\frac{1}{r}\frac{\partial}{\partial r}+\frac{\partial^2}{\partial z^2}+\alpha^2\right)P=0.$$

This can then be factored and an equation derived to describe either forward propagation, if it is positive, or backward propagation, if it is negative, as

$$\frac{du}{dr}=\pm i\sqrt{\frac{\partial^2 u}{\partial z^2}+\alpha^2 u}$$

where $\alpha$ is defined to be

$$\alpha=\frac{\omega}{c(r,z)}.$$

Here, $\omega$ is angular frequency and $c$ is the sound speed written in terms of the range which will model time, $r$, and depth, $z$. The solution $u$ to this "one way equation" is related to the solution, $P$, from the Helmholtz equation by the change of variable equation

$$u=\sqrt{r}P.$$

This partial differential equation involves the square root of an operator. Taking the square root of an operator makes it very difficult to solve numerically using ordinary methods because you would discretize the operator by a matrix and then approximate the square root of the matrix which is computationally expensive. A better approach would be to find accurate eigenvalues and eigenfunctions of the operator because then it is trivial to solve. The operator here, $\frac{\partial^2 u}{\partial z^2}+\alpha^2 u$, has the form of a Schrödinger operator discussed in Chapter 1. It is the Laplacian operator with a coefficient of 1 and the coefficient $\alpha^2$ is considered a potential in this case.

The coefficient $\alpha$ is piecewise constant in this case because as the depth of the ocean changes, the wavenumber will change. For this project, we are assuming the coefficient $\alpha$ has three pieces. The first and last piece are constant and as discussed before, we can average the second piece because it is nearly constant. The piecewise function results in discontinuities where the frequency changes at the interfaces of where the sound speed

changes. My previous research done with Lambers has proven that solution methods using eigenfunction expansion have been effective in solving piecewise constant PDEs [12]. It will be shown that natural frequencies at the discontinuities can be found and eigenfunctions constructed to characterize the solution. This project differs from the previous research in that the "one way equation" has a different operator, the Schrödinger operator, and the boundary conditions for this problem are Dirichlet as opposed to periodic.

## 2.1 Previous Work

Similar to previous research with eigenfunction expansion, we will begin by defining the eigenfunctions as combinations of sine and cosine functions. Each eignefunction has conditions such as the boundary conditions and continuity requirements at the interfaces of the pieces. The system of equations can then be reduced by eliminating the parameters that come from frequency, amplitude, and phase shifts. Once the system is reduced to a nonlinear equation we can solve for the remaining variable using the secant method [4]. This method has been used previously to solve for the natural frequency and allow us to construct the solution [7]. In order to use The Secant Method, initial guesses of the natural frequency must be found by using a good approximation of the eigenfunction.

## 2.2 Challenges

The difficulty of this project will come as we increase the spatial resolution in order to accurately solve problems that model our real-world experiences. Increasing the spatial resolution increases the number of eigenvalues. Figure 2.1 is the graph of the absolute value of all of the eigenvalues. The first three are positive eigenvalues that are bounded in magnitude; however, the remaining eigenvalues are negative and go to negative infinity. We will see that as more eigenvalues are introduced, the smaller and particularly the positive eigenvalues result in eigenfunctions that behave very differently from one another.

Figure 2.2 displays the eigenfunction in blue and the function $\sin(\frac{jx}{2})$ in red. We can see that eigenfunctions that correspond to negative eigenvalues can be approximated by a sine function; however, as the eigenvalues approach 0, they become more difficult to approximate using that sine function. In fact, when the eigenvalues become positive they nowhere resemble a sine function as we can see from Figure 2.2, so we must therefore develop a different approach for approximating these eigenfunctions.

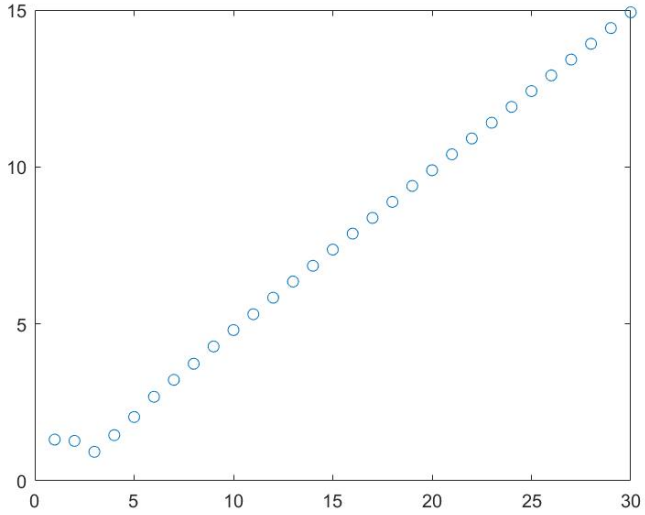


*Figure 2.1*: Graph of the absolute values of all eigenvalues of "one way" equation

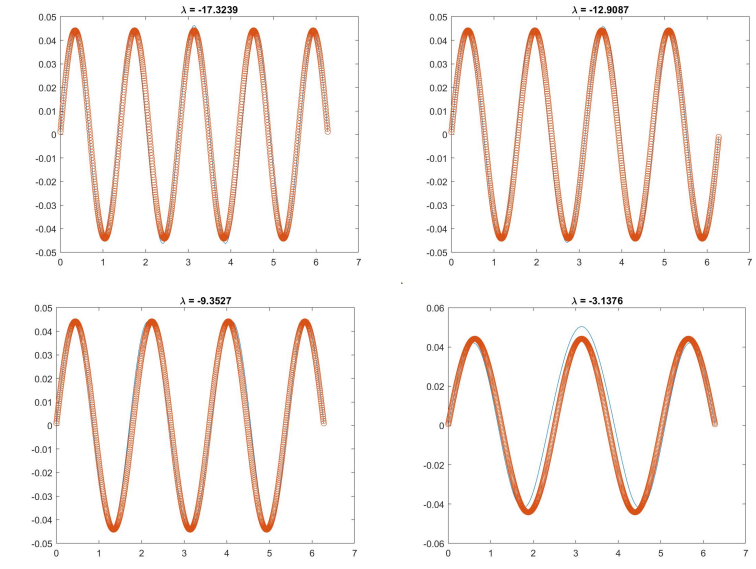


*Figure 2.2*: Eigenfunctions that correspond to negative eigenvalues compared to the function $\sin(\frac{jx}{2})$.

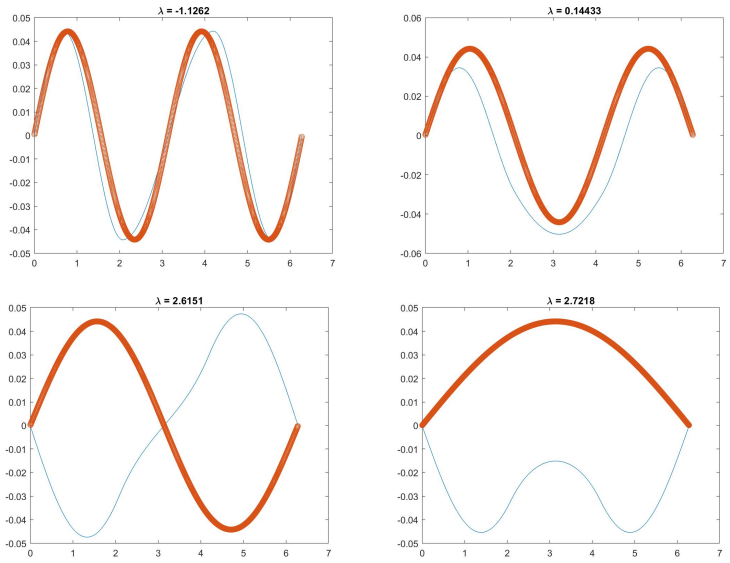


*Figure 2.3*: Eigenfunctions that correspond to positive eigenvalues compared to the function $\sin(\frac{jx}{2})$.

# Chapter 3

# Methodology

## 3.1 Approach

In order to understand the approach taken to find all of the eigenfunctions from both the positive and negative eigenvalues, first we will look at the system of equations used to characterize the eigenfunction solution.

The eigenfunctions for the piecewise constant coefficient case will be described by:

$$V_j(x) = \begin{cases} A_1\cos(\omega_1 x) + B_1\sin(\omega_1 x) & 0 \le x < 2\pi\rho_1 \\ A_2\cos(\omega_2 x) + B_2\sin(\omega_2 x) & 2\pi\rho_1 \le x < 2\pi\rho_2 \\ A_3\cos(\omega_3 x) + B_3\sin(\omega_3 x) & 2\pi\rho_2 \le x < 2\pi \end{cases}$$

where $\omega_{j1}, ..., \omega_{j3}$ are the frequencies and $A_{j1}, A_{j2}, A_{j3}$ and $B_{j1}, B_{j2}, B_{j3}$ represent the unknown amplitudes and phase shifts.

This system comes from imposing conditions on the eigenfunctions generated from the trigonometric equation. The spatial domain for the eigenfunctions is from 0 to $2\pi$ and we are specifically looking at the 3-piece case where $\rho_1$ and $\rho_2$ define the interfaces of the pieces. The conditions that we will impose come from the Dirichlet boundary conditions, meaning the solution is zero at the endpoints. The other equations come from the continuity requirements. This means that the one-sided limits of eigenfunctions at the interface are equal as well as their derivatives [13]. We will also set conditions for how $\omega_1$, $\omega_2$, and $\omega_3$ relate to each other on the different pieces.

Dirichlet Boundary Conditions:

$$V_{j1}(0) = 0 \tag{3.1}$$

$$V_{jn}(0) = 0 \tag{3.2}$$

Continuity:

$$V_{j1}(2\pi\rho_1) = V_{j2}(2\pi\rho_1) \tag{3.3}$$

$$V'_{j1}(2\pi\rho_1) = V'_{j2}(2\pi\rho_1) \tag{3.4}$$

$$V_{j2}(2\pi\rho_2) = V_{j3}(2\pi\rho_2) \tag{3.5}$$

$$V'_{j2}(2\pi\rho_2) = V'_{j3}(2\pi\rho_2) \tag{3.6}$$

This leads to the homogeneous system of equations for the coefficients $A_i$ and $B_i$. From the boundary conditions we have

$$A_1 \cos(\omega_1(0)) + B_1 \sin(\omega_1(0)) = 0 \tag{3.7}$$

$$A_1 = 0 \tag{3.8}$$

and

$$A_3 \cos(\omega_3(2\pi)) + B_3 \sin(\omega_3(2\pi)) = 0 \tag{3.9}$$

We see that $A_1$ is 0. From the continuity requirements we have

$$\begin{aligned} A_1 \cos(\omega_1 2\pi\rho_1) + B_1 \sin(\omega_1 2\pi\rho_1) &= A_2 \cos(\omega_2 2\pi\rho_1) \\ &\quad + B_2 \sin(\omega_2 2\pi\rho_1) \end{aligned} \tag{3.10}$$

$$\begin{aligned} -\omega_1 A_1 \sin(\omega_1 2\pi\rho_1) + \omega_1 B_1 \cos(\omega_1 2\pi\rho_1) &= -\omega_1 A_2 \sin(\omega_2 2\pi\rho_1) \\ &\quad + \omega_2 B_2 \cos(\omega_2 2\pi\rho_1) \end{aligned} \tag{3.11}$$

$$\begin{aligned} A_2 \cos(\omega_2 2\pi\rho_2) + B_2 \sin(\omega_2 2\pi\rho_2) &= A_3 \cos(\omega_3 2\pi\rho_2) \\ &\quad + B_3 \sin(\omega_3 2\pi\rho_2) \end{aligned} \tag{3.12}$$

$$\begin{aligned} -\omega_2 A_2 \sin(\omega_2 2\pi\rho_2) + \omega_2 B_2 \cos(\omega_2 2\pi\rho_2) &= -\omega_3 A_3 \sin(\omega_3 2\pi\rho_2) \\ &\quad + \omega_3 B_3 \cos(\omega_3 2\pi\rho_2) \end{aligned} \tag{3.13}$$

and the $\omega$ relations

$$-\omega_1^2 + \alpha_1^2 = -\omega_3^2 + \alpha_3^2$$

$$-\omega_2^2 + \alpha_2^2 = -\omega_3^2 + \alpha_3^2$$

give us:

$$\omega_1 = \sqrt{\omega_3^2 - \alpha_3^2 + \alpha_1^2} \tag{3.14}$$

$$\omega_2 = \sqrt{\omega_3^2 - \alpha_3^2 + \alpha_2^2} \tag{3.15}$$

The system of equations from the continuity requirements results in a block lower triangular matrix with a rank-2 update. The entries of this matrix, which we will call $M$, come from the coefficients of $A_i$ and $B_i$ from the system of equations.

$$M = \begin{bmatrix} A & B \\ C & D \end{bmatrix}$$

where

$$A = \begin{bmatrix} 0 \end{bmatrix}$$

$$B = \begin{bmatrix} 0 & 0 & \cos(2\pi\omega_3) & \sin(2\pi\omega_3) \end{bmatrix}$$

$$C = \begin{bmatrix} \sin(2\pi\rho_1\omega_1) \\ \omega_1(\cos(2\pi\rho_1\omega_1)) \\ 0 \\ 0 \end{bmatrix}$$

$$D = \begin{bmatrix} -\cos(2\pi\rho_1\omega_2) & -\sin(2\pi\rho_1\omega_2) & 0 & 0 \\ \omega_2(\sin(2\pi\rho_1\omega_2)) & -\omega_2(\cos(2\pi\rho_1\omega_2)) & 0 & 0 \\ \cos(2\pi\rho_2\omega_2) & \sin(2\pi\rho_2\omega_2) & -\cos(\omega_3 2\pi\rho_2) & -\sin(\omega_3 2\pi\rho_2) \\ -\omega_2(\sin(2\pi\rho_2\omega_2)) & \omega_2(\cos(2\pi\rho_2\omega_2) & \omega_3\sin(\omega_3 2\pi\rho_2) & -\omega_3\cos(\omega_3 2\pi\rho_2) \end{bmatrix}$$

An important aspect of our method will be that we find a value for $\omega_3$ to ensure the matrix is singular, meaning the determinant of the matrix is zero and therefore the system of equations has a non-zero solution [10]. To solve for the $\omega_3$ value, we need an equation for the determinant.

$$\det(M) = \det(A - BD^{-1}C)\det(D) \tag{3.16}$$

We can prove that the determinant of the block $D$ is always non-zero, and thus we will proceed to find the value of $\omega_3$ by looking at $\det(A - BD^{-1}C)$ [10]. The Secant Method will be used to determine the value for $\omega_3$; however, in order to use The Secant Method, we must have two initial guesses.

For sufficiently large $j$ values, we have seen that $\sin(\frac{jx}{2})$ is a good approximation of the eigenfunction of $L$. In order to obtain an approximate $\omega_3$ value, we will use the Rayleigh Quotient

$$R(L, V_j) = \frac{\langle V_j, LV_j \rangle}{\langle V_j, V_j \rangle} \tag{3.17}$$

where $L$ is our operator being applied to the eigenfunction $V_j$. The Rayleigh Quotient is a good approximation for the exact eigenvalue $\lambda$ for sufficiently large $j$ values. This gives us the equation

$$\lambda = \frac{\langle \sin(\frac{jx}{2}), L\sin(\frac{jx}{2}) \rangle}{\langle \sin(\frac{jx}{2}), \sin(\frac{jx}{2}) \rangle} \tag{3.18}$$

Since

$$\lambda = -\omega_i^2 + \alpha_i^2, \tag{3.19}$$

we can set the right side of this equation equal to the Rayleigh Quotient

$$\frac{\langle \sin(\frac{jx}{2}), L\sin(\frac{jx}{2})\rangle}{\langle \sin(\frac{jx}{2}), \sin(\frac{jx}{2})\rangle} = -\omega_i^2 + \alpha_i^2 \tag{3.20}$$

and solve for $\omega_i$ which will be our initial guess to use for the Secant Method.

To find an initial guess for the $\omega_3$ value corresponding to the positive eigenvalues we will need another approach. As Figure 2.2 from Chapter 2 showed us, the function $\sin(\frac{jx}{2})$ is not a good approximation of our eigenfunction. We will let $\phi_1, \phi_2, \ldots, \phi_J$ represent the inaccurate approximations of $\phi_k(x) = \sin(\frac{kx}{2})$. So we can call the subspace spanned by the inaccurate sine approximations

$$\Phi_J = \text{span}\{\phi_1, \ldots, \phi_J\}.$$

The orthogonal projection $P_J$ of a function $u$ into $\Phi_J$ is defined by

$$P_J u = \sum_{j=1}^{J} \frac{\phi_j \langle\, \phi_j, u\rangle}{\langle\, \phi_j, \phi_j\rangle}.$$

Then, the restriction of the operator $L$ to $\phi_J$ is defined by

$$L_J = P_J L P_J.$$

We will construct the matrix $A_0$ such that its entries $a_{ij}$ are computed by

$$a_{ij} = \frac{\langle\, \phi_i, L\phi_j\rangle}{\langle\, \phi_i, \phi_i\rangle}.$$

$A_0$ is the matrix of the restriction in the basis of the subspace $\Phi_J$.

The matrix entries for $i \neq j$ are

$$[A_0]_{ij} = \frac{\int_0^{2\pi} \phi_i(x)\left(\frac{\partial^2}{\partial(x)^2} + \alpha^2(x)\right)\phi_j(x)dx}{\sqrt{\int_0^{2\pi}\phi_i^2(x)dx \int_0^{2\pi}\phi_j^2(x)dx}}.$$

Because $\phi_n(x) = \sin(\frac{nx}{2})$ and $L\phi_n = -(\frac{n}{2})^2\sin(\frac{nx}{2}) + \alpha(x)^2\sin(\frac{nx}{2})$, then we can rewrite the entries.

$$[A_0]_{ij} = \frac{\int_0^{2\pi}\left(\sin(\frac{ix}{2})\right)\left(-(\frac{j}{2})^2\sin(\frac{jx}{2}) + \alpha(x)^2\sin(\frac{jx}{2})\right)dx}{\int_0^{2\pi}\sin(\frac{jx}{2})\sin(\frac{jx}{2})dx} \tag{3.21}$$

$$= \frac{\int_0^{2\pi} -(\frac{j}{2})^2\sin(\frac{ix}{2})\sin(\frac{jx}{2})dx + \int_0^{2\pi}\alpha(x)^2\sin(\frac{ix}{2})\sin(\frac{jx}{2})dx}{\pi} \tag{3.22}$$

$$= \frac{-(\frac{j}{2})^2\int_0^{2\pi}\sin(\frac{ix}{2})\sin(\frac{jx}{2})dx + \int_0^{2\pi}\alpha(x)^2\sin(\frac{ix}{2})\sin(\frac{jx}{2})dx}{\pi} \tag{3.23}$$

Using the trig identity $\sin(u)\sin(v) = \frac{1}{2}[\cos(u-v) - \cos(u+v)]$ where $u = \frac{ix}{2}$ and $v = \frac{jx}{2}$

$$\begin{aligned}
[A_0]_{ij} &= \frac{-(\frac{j}{2})^2 \int_0^{2\pi} \frac{1}{2}\left[\cos(\frac{ix}{2} - \frac{jx}{2}) - \cos(\frac{ix}{2} + \frac{jx}{2})\right] dx}{\pi} \\
&+ \frac{\int_0^{2\pi} \alpha(x)^2 \frac{1}{2}\left[\cos(\frac{ix}{2} - \frac{jx}{2}) - \cos(\frac{ix}{2} + \frac{jx}{2})\right] dx}{\pi} \qquad (3.24) \\
&= \frac{-(\frac{j^2}{8}) \int_0^{2\pi} \left[\cos(\frac{ix}{2} - \frac{jx}{2}) - \cos(\frac{ix}{2} + \frac{jx}{2})\right] dx}{\pi} \qquad (3.25) \\
&+ \frac{\frac{\alpha(x)^2}{2} \int_0^{2\pi} \left[\cos(\frac{ix}{2} - \frac{jx}{2}) - \cos(\frac{ix}{2} + \frac{jx}{2})\right] dx}{\pi} \qquad (3.26)
\end{aligned}$$

We will look at the individual integrals from Equation 3.25 and 3.26 above in order to simplify.

From the first part in (3.25) we have

$$\begin{aligned}
&\int_0^{2\pi} \left[\cos\left(\frac{ix}{2} - \frac{jx}{2}\right) - \cos\left(\frac{ix}{2} + \frac{jx}{2}\right)\right] dx \\
&= \int_0^{2\pi} \cos\left(\frac{ix}{2} - \frac{jx}{2}\right) dx - \int_0^{2\pi} \cos\left(\frac{ix}{2} + \frac{jx}{2}\right) dx
\end{aligned}$$

Using u-substitution for each integral where

$$u = \frac{ix}{2} - \frac{jx}{2}, \quad du = \frac{i-j}{2} dx, \quad dx = \frac{2du}{i-j}$$

for the first integral and

$$u = \frac{ix}{2} + \frac{jx}{2}, \quad du = \frac{i+j}{2} dx, \quad dx = \frac{2du}{i+j}$$

for the second integral,

$$\begin{aligned}
\int_0^{2\pi} \cos\left(\frac{ix}{2} - \frac{jx}{2}\right) dx &- \int_0^{2\pi} \cos\left(\frac{ix}{2} + \frac{jx}{2}\right) dx \\
&= \frac{2}{i-j} \int_0^{i\pi - j\pi} \cos(u) du - \frac{2}{i+j} \int_0^{i\pi + j\pi} \cos(u) du \\
&= \frac{2}{i-j} [\sin(u)]_0^{i\pi - j\pi} - \frac{2}{i+j} [\sin(u)]_0^{i\pi + j\pi} \\
&= \frac{2}{i-j} [\sin(i\pi - j\pi) - \sin(0)] - \frac{2}{i+j} [\sin(i\pi + j\pi) - \sin(0)] \\
&= \frac{2\sin(i\pi - j\pi)}{i-j} - \frac{2\sin(i\pi + j\pi)}{i+j} \\
&= 2\left[\frac{(i+j)\sin(i\pi - j\pi) - (i-j)\sin(i\pi + j\pi)}{i^2 - j^2}\right] \qquad (3.27)
\end{aligned}$$

Now the second integral involving $\alpha$ from part (3.26) is

$$\frac{\alpha(x)^2}{2}\int_0^{2\pi}\left[\cos\left(\frac{ix}{2}-\frac{jx}{2}\right)-\cos\left(\frac{ix}{2}+\frac{jx}{2}\right)\right]dx.$$

Since the coefficient $\alpha$ is piecewise constant, this integral is the sum of the integrals corresponding to each of the three pieces.

$$\begin{aligned}\frac{\alpha(x)^2}{2}\int_0^{2\pi} &\left[\cos\left(\frac{ix}{2}-\frac{jx}{2}\right)-\cos\left(\frac{ix}{2}+\frac{jx}{2}\right)\right]dx = \\ &\frac{\alpha_1(x)^2}{2}\int_0^{2\pi\rho_1}\left[\cos\left(\frac{ix}{2}-\frac{jx}{2}\right)-\cos\left(\frac{ix}{2}+\frac{jx}{2}\right)\right]dx+ \\ &\frac{\alpha_2(x)^2}{2}\int_{2\pi\rho_1}^{2\pi\rho_2}\left[\cos\left(\frac{ix}{2}-\frac{jx}{2}\right)-\cos\left(\frac{ix}{2}+\frac{jx}{2}\right)\right]dx+ \\ &\frac{\alpha_3(x)^2}{2}\int_{2\pi\rho_2}^{2\pi}\left[\cos\left(\frac{ix}{2}-\frac{jx}{2}\right)-\cos\left(\frac{ix}{2}+\frac{jx}{2}\right)\right]dx \end{aligned} \tag{3.28}$$

This simplifies to

$$\begin{aligned}&\alpha_1(x)^2\left[\frac{(i+j)\sin(\rho_1(i\pi-j\pi))-(i-j)\sin(\rho_1(i\pi+j\pi))}{i^2-j^2}\right]+ \\ &\alpha_2(x)^2\left[\frac{(i+j)\sin(\rho_2(i\pi-j\pi))-(i+j)\sin(\rho_1(i\pi-j\pi))}{i^2-j^2}\right. \\ &\left.\frac{-(i-j)\sin(\rho_2(i\pi+j\pi))+(i-j)\sin(\rho_1(i\pi+j\pi))}{i^2-j^2}\right]+ \\ &\alpha_3(x)^2\left[\frac{(i+j)\sin(i\pi-j\pi)-(i+j)\sin(\rho_2(i\pi-j\pi))}{i^2-j^2}\right. \\ &\left.\frac{-(i-j)\sin(i\pi+j\pi)+(i-j)\sin(\rho_2(i\pi+j\pi))}{i^2-j^2}\right]\end{aligned} \tag{3.29}$$

Since the sine of any integer multiple of $\pi$ is zero, and $i$ and $j$ are both integers this becomes

$$\begin{aligned}&\alpha_1(x)^2\left[\frac{(i+j)\sin(\rho_1(i\pi-j\pi))-(i-j)\sin(\rho_1(i\pi+j\pi))}{i^2-j^2}\right]+ \\ &\alpha_2(x)^2\left[\frac{(i+j)\sin(\rho_2(i\pi-j\pi))-(i+j)\sin(\rho_1(i\pi-j\pi))}{i^2-j^2}\right. \\ &\left.\frac{-(i-j)\sin(\rho_2(i\pi+j\pi))+(i-j)\sin(\rho_1(i\pi+j\pi))}{i^2-j^2}\right]+ \\ &\alpha_3(x)^2\left[\frac{-(i+j)\sin(\rho_2(i\pi-j\pi))+(i-j)\sin(\rho_2(i\pi+j\pi))}{i^2-j^2}\right].\end{aligned} \tag{3.30}$$

Now that we have simplified both of the integrals from part (3.25) and (3.26) in order to obtain the simplified equation for the entries to matrix $A_0$, we will substitute Equation (3.27) into part (3.25) and Equation (3.30), which we will call $X$, into part (3.26).

$$\frac{-(\frac{j^2}{8})2\left[\frac{(i+j)\sin(i\pi-j\pi)-(i-j)\sin(i\pi+j\pi)}{i^2-j^2}\right]+X}{\pi}$$

After simplifying the sine terms that equal 0, we have the final equation for the matrix entries when $i \neq j$

$$[A_0]_{ij} = \frac{X}{\pi}.$$

For the $i = j$ case:

$$[A_0]_{ij} = \frac{\langle \phi_j, L\phi_j \rangle}{\langle \phi_j, \phi_j \rangle} = -\left(\frac{j}{2}\right)^2 + \frac{1}{\pi}\int_0^{2\pi} \alpha(x)^2 \sin^2\left(\frac{jx}{2}\right) dx$$

Expanding the alpha term:

$$[A_0]_{ij} = -\left(\frac{j}{2}\right)^2 + \frac{1}{\pi}B$$

where

$$\begin{aligned} B &= \alpha_1^2\left[-\frac{\sin(2\pi\rho_1 j) - 2\pi\rho_1 j}{2j}\right] + \\ &\quad \alpha_2^2\left[-\frac{\sin(2\pi\rho_2 j) - 2\pi\rho_2 j - \sin(2\pi\rho_1 j) + 2\pi\rho_1 j}{2j}\right] \\ &+ \alpha_3^2\left[\pi + \frac{\sin(2\pi\rho_2 j) - 2\pi\rho_2 j}{2j}\right]. \end{aligned} \tag{3.31}$$

Now that we have formulas to find initial guesses for the values of $j$ that can be approximated using $\sin(\frac{jx}{2})$ and the matrix $A_0$, we also need a way to evaluate the cutoff value of $j$ that will tell us for what values of $j$ the initial guesses will come from what method. We know the majority of our initial guesses can be found by using $\sin(\frac{jx}{2})$, so we will test for the values of $j$ that cannot be approximated using this.

Use Error formula to find bad $j$ values

$$E_j = \frac{\langle L\phi_j, L\phi_j \rangle - \mu_j^2 \langle \phi_j, \phi_j \rangle}{\langle L\phi_j, L\phi_j \rangle}$$

where

$$\mu_j = \frac{\langle \phi_j, L\phi_j \rangle}{\langle \phi_j, \phi_j \rangle}$$

$$E_j = \frac{\int_0^{2\pi} \alpha(x)^4 \sin^2\left(\frac{jx}{2}\right) dx - \frac{1}{\pi}\left[\int_0^{2\pi} \alpha(x)^2 \sin^2\left(\frac{jx}{2}\right) dx\right]^2}{(\frac{j}{2})^4\pi - \frac{j^2}{2}\int_0^{2\pi} \alpha(x)^2 \sin^2(\frac{jx}{2})\,dx + \int_0^{2\pi} \alpha(x)^4 \sin^2(\frac{jx}{2})\,dx} \tag{3.32}$$

$$= \frac{A - \frac{1}{\pi}B^2}{(\frac{j}{2})^4\pi - \frac{j^2}{2}B + A} \tag{3.33}$$

where

$$A = \alpha_1^4 \int_0^{2\pi\rho_1} \sin^2(\frac{jx}{2})\,dx + \alpha_2^4 \int_{2\pi\rho_1}^{2\pi\rho_2} \sin^2(\frac{jx}{2})\,dx + \alpha_3^4 \int_{2\pi\rho_2}^{2\pi} \sin^2(\frac{jx}{2})\,dx \tag{3.34}$$

$$B = \alpha_1^2 \int_0^{2\pi\rho_1} \sin^2(\frac{jx}{2})\,dx + \alpha_2^2 \int_{2\pi\rho_1}^{2\pi\rho_2} \sin^2(\frac{jx}{2})\,dx + \alpha_3^2 \int_{2\pi\rho_2}^{2\pi} \sin^2(\frac{jx}{2})\,dx \tag{3.35}$$

Finding the definite integrals and combining,

$$\begin{aligned} A = {} & \alpha_1^4\left[-\frac{\sin(2\pi\rho_1 j) - 2\pi\rho_1 j}{2j}\right] \\ & + \alpha_2^4\left[-\frac{\sin(2\pi\rho_2 j) - 2\pi\rho_2 j - \sin(2\pi\rho_1 j) + 2\pi\rho_1 j}{2j}\right] \\ & + \alpha_3^4\left[\pi + \frac{\sin(2\pi\rho_2 j) - 2\pi\rho_2 j}{2j}\right] \end{aligned} \tag{3.36}$$

$$\begin{aligned} B = {} & \alpha_1^2\left[-\frac{\sin(2\pi\rho_1 j) - 2\pi\rho_1 j}{2j}\right] \\ & + \alpha_2^2\left[-\frac{\sin(2\pi\rho_2 j) - 2\pi\rho_2 j - \sin(2\pi\rho_1 j) + 2\pi\rho_1 j}{2j}\right] \\ & + \alpha_3^2\left[\pi + \frac{\sin(2\pi\rho_2 j) - 2\pi\rho_2 j}{2j}\right] \end{aligned} \tag{3.37}$$

Using this error formula will allow us to find the values of $j$ that need to use the matrix $A_0$ to find the initial guesses. The initial guesses of $\omega_3$ found for all values of $j$ are passed through the Secant Method in order to obtain our true $\omega_3$ values. Then the eigenvalues, $\lambda$, can be found by

$$\lambda = -\omega_3^2 + \alpha_3^2$$

Then the matrix $M$ is constructed using the $\omega_3$ value found such that the matrix is singular. The null space of $M$ is found in order to solve for the coefficients of our eigenfunction. The

values of $\omega_1$ and $\omega_2$ can be found using the $\omega$ relations previously described. Taking all of this information, the eigenfunction

$$V_j(x) = \begin{cases} A_1\cos(\omega_1 x) + B_1\sin(\omega_1 x) & 0 \le x < 2\pi\rho_1 \\ A_2\cos(\omega_2 x) + B_2\sin(\omega_2 x) & 2\pi\rho_1 \le x < 2\pi\rho_2 \\ A_3\cos(\omega_3 x) + B_3\sin(\omega_3 x) & 2\pi\rho_2 \le x < 2\pi \end{cases}$$

can be constructed for each value of $j$. The eigenfunction expansion is put together by adding all of the eigenfunctions found from the $j$ values.

# Chapter 4

# Numerical Results

The following numerical results were obtained by using the eigenfunction expansion method described in the previous chapter, which we will call EigExp, to test its efficiency by running it with three different final times ($t_f$): 0.01, 0.1, and 1. For each final time constraint, the method was tested using the different grid sizes 1023, 2047, and 4095. For each test, the information collected included the time it took to compute the solution as well as how many terms were needed. Each test was run using either $\sin(2x)$ or a characteristic function as initial data. The piecewise constant $\alpha$ and the value of the interface, $\rho$, varied between trials as well. For $\alpha^1$, the value of the pieces were $[2,1,2]$ and the values for $\rho$ were $[\frac{1}{3},\frac{2}{3}]$. For $\alpha^2$, the value of the pieces were $[1,2,3]$ and the values for $\rho$ were $[\frac{1}{4},\frac{3}{4}]$. For $\alpha^3$, the value of the pieces were $[2,1,3]$ and the values for $\rho$ were $[\frac{1}{4},\frac{1}{2}]$.

This method was then compared to the Crank-Nicolson method to test the time it took to compute. Crank-Nicolson is a finite difference method based on the trapezoidal rule. It is unconditionally stable and a good method to compare against. The method was also compared to MATLAB's ODE solver called `ode15s`. This is used with stiff problems and has low to medium accuracy because it works well with differential algebraic equations. Looking at the tables and graphs, we can see that the eigenfunction expansion method performed consistently better with all of the parameters and was able to scale to higher resolutions more efficiently while the other methods had higher error values.

| $\alpha^1$, $sin2x$ | | | | | | |
|---|---|---|---|---|---|---|
| | | EigExp | | C-N | `ode15s` | |
| $t_f$ | $N$ | time | terms | time | time | $\Delta t_{\text{avg}}$ |
| 0.01 | 1023 | 0.112 | 75 | 0.028 | 0.099 | 7.692e-04 |
| | 2047 | 0.015 | 75 | 0.009 | 0.018 | 7.143e-04 |
| | 4095 | 0.022 | 75 | 0.021 | 0.042 | 6.667e-04 |
| 0.1 | 1023 | 0.007 | 24 | 0.007 | 0.053 | 3.226e-03 |
| | 2047 | 0.011 | 24 | 0.014 | 0.066 | 3.226e-03 |
| | 4095 | 0.012 | 24 | 0.018 | 0.123 | 3.030e-03 |
| 1 | 1023 | 0.005 | 9 | 0.006 | 0.048 | 1.818e-02 |
| | 2047 | 0.004 | 9 | 0.012 | 0.094 | 1.786e-02 |
| | 4095 | 0.006 | 9 | 0.019 | 0.149 | 1.724e-02 |

*Table 4.1*:

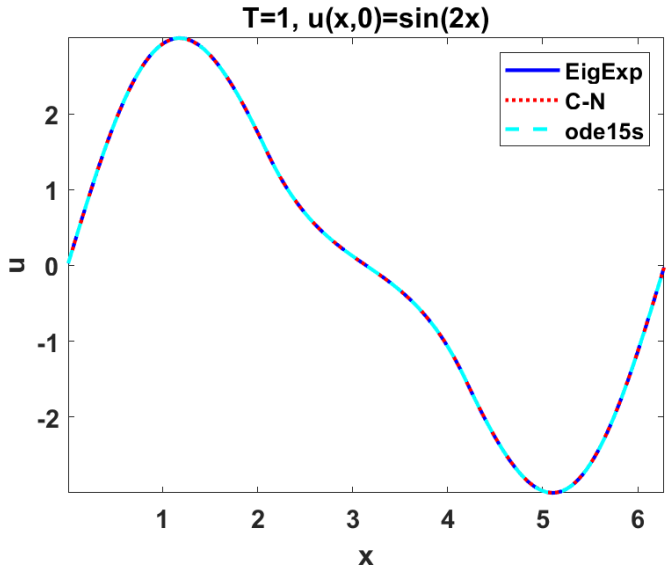


*Figure 4.1*: Graph with initial data $\sin 2x$ with 1023 grid points using the coefficient $\alpha^1$ with a final time of $10^{-0}$

| $\alpha^1$, CharFunc | | | | | | |
|---|---|---|---|---|---|---|
| | | EigExp | | C-N | `ode15s` | |
| $t_f$ | $N$ | time | terms | time | time | $\Delta t_{\text{avg}}$ |
| 0.01 | 1023 | 0.011 | 75 | 0.005 | 0.081 | 1.053e-04 |
| | 2047 | 0.015 | 75 | 0.011 | 0.144 | 8.929e-05 |
| | 4095 | 0.027 | 75 | 0.020 | 0.342 | 7.692e-05 |
| 0.1 | 1023 | 0.005 | 24 | 0.005 | 0.092 | 8.065e-04 |
| | 2047 | 0.014 | 24 | 0.012 | 0.188 | 7.042e-04 |
| | 4095 | 0.008 | 24 | 0.018 | 0.391 | 6.289e-04 |
| 1 | 1023 | 0.005 | 9 | 0.005 | 0.092 | 6.536e-03 |
| | 2047 | 0.006 | 9 | 0.011 | 0.191 | 5.848e-03 |
| | 4095 | 0.006 | 9 | 0.026 | 0.583 | 5.319e-03 |

*Table 4.2*:

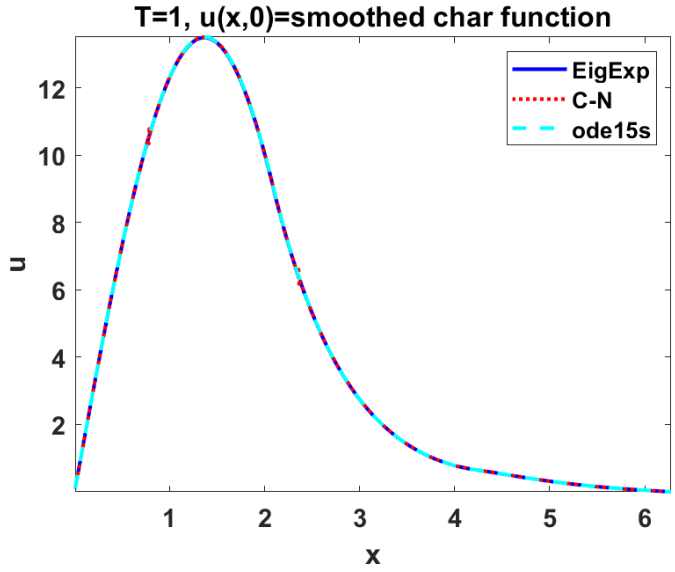


*Figure 4.2*: Graph with initial data from the characteristic function with 1023 grid points using the coefficient $\alpha^1$ with a final time of $10^{-0}$

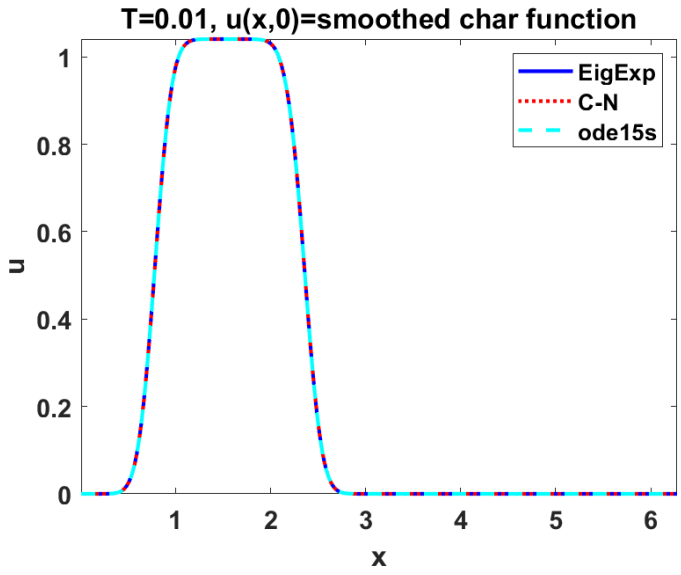


*Figure 4.3*: Graph with initial data from the characteristic function with 1023 grid points using the coefficient $\alpha^1$ with a final time of $10^{-2}$

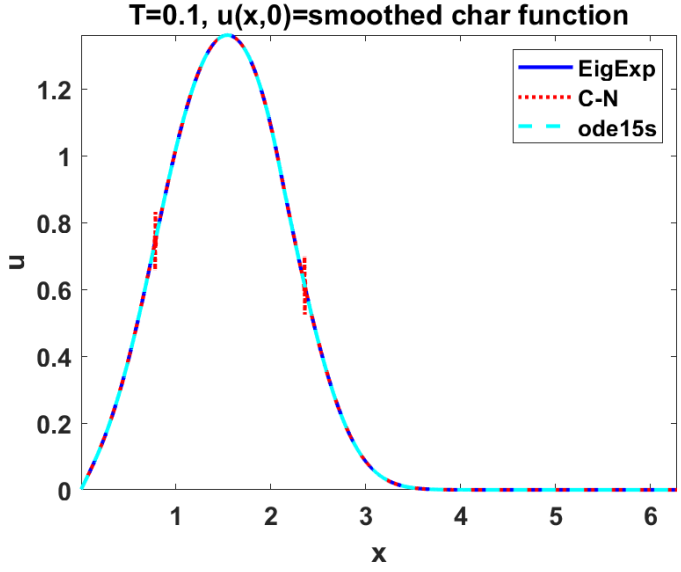


*Figure 4.4*: Graph with initial data from the characteristic function with 2047 grid points using the coefficient $\alpha^1$ with a final time of $10^{-1}$. We see that Crank Nicholson did not scale well.

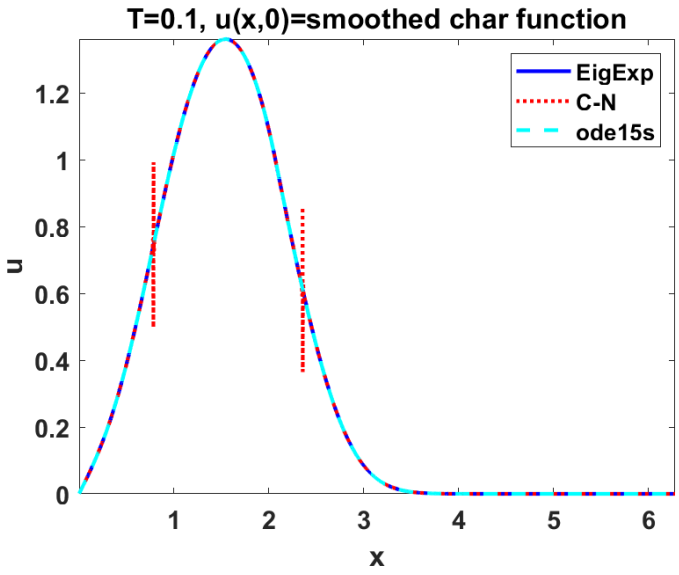


*Figure 4.5*: Graph with initial data from the characteristic function with 4095 grid points using the coefficient $\alpha^1$ with a final time of $10^{-1}$. We see that the Eigenfunction Expansion method worked well when the gridpoints were scaled whereas the other methods did not.

| $\alpha^2$, $Sin2x$ | | | | | | |
|---|---|---|---|---|---|---|
| | | EigExp | | C-N | `ode15s` | |
| $t_f$ | $N$ | time | terms | time | time | $\Delta t_{\text{avg}}$ |
| 0.01 | 1023 | 0.056 | 75 | 0.005 | 0.023 | 4.348e-04 |
| | 2047 | 0.019 | 75 | 0.011 | 0.033 | 4.348e-04 |
| | 4095 | 0.024 | 75 | 0.020 | 0.073 | 4.167e-04 |
| 0.1 | 1023 | 0.008 | 24 | 0.007 | 0.030 | 2.564e-03 |
| | 2047 | 0.010 | 24 | 0.011 | 0.053 | 2.439e-03 |
| | 4095 | 0.010 | 24 | 0.020 | 0.139 | 2.326e-03 |
| 1 | 1023 | 0.005 | 9 | 0.005 | 0.052 | 1.408e-02 |
| | 2047 | 0.006 | 9 | 0.013 | 0.099 | 1.370e-02 |
| | 4095 | 0.006 | 9 | 0.025 | 0.194 | 1.351e-02 |

*Table 4.3*:

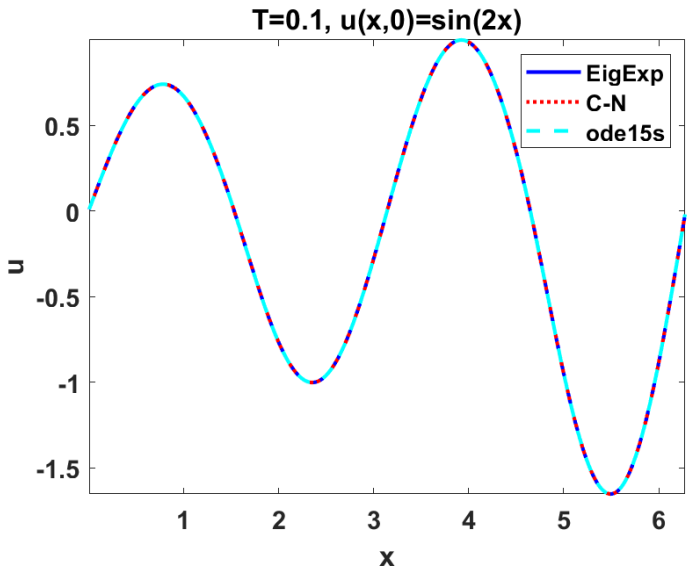


*Figure 4.6*: Graph with initial data $sin2x$ with 1023 grid points using the coefficient $\alpha^2$ with a final time of $10^{-1}$

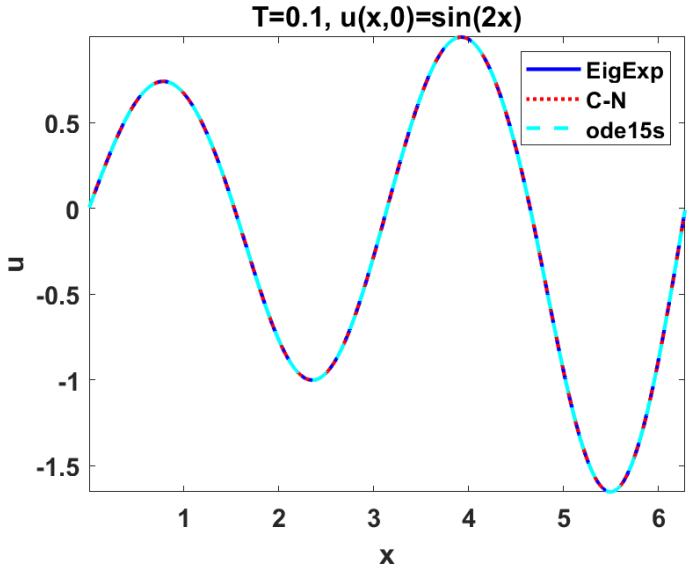


*Figure 4.7*: Graph with initial data $sin2x$ with 2047 grid points using the coefficient $\alpha^2$ with a final time of $10^{-1}$

| $\alpha^2$, CharFunc | | | | | | |
|---|---|---|---|---|---|---|
| | | EigExp | | C-N | `ode15s` | |
| $t_f$ | $N$ | time | terms | time | time | $\Delta t_{\text{avg}}$ |
| 0.01 | 1023 | 0.018 | 75 | 0.005 | 0.049 | 1.053e-04 |
| | 2047 | 0.034 | 75 | 0.012 | 0.158 | 8.929e-05 |
| | 4095 | 0.031 | 75 | 0.021 | 0.325 | 7.692e-05 |
| 0.1 | 1023 | 0.009 | 24 | 0.006 | 0.076 | 8.000e-04 |
| | 2047 | 0.006 | 24 | 0.010 | 0.139 | 7.042e-04 |
| | 4095 | 0.014 | 24 | 0.020 | 0.436 | 6.250e-04 |
| 1 | 1023 | 0.003 | 9 | 0.006 | 0.113 | 6.211e-03 |
| | 2047 | 0.007 | 9 | 0.011 | 0.218 | 5.618e-03 |
| | 4095 | 0.010 | 9 | 0.025 | 0.471 | 5.102e-03 |

*Table 4.4*:

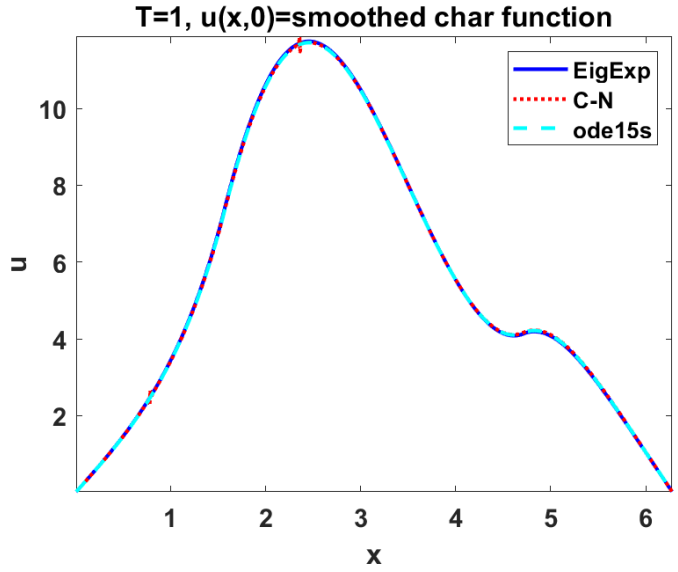


*Figure 4.8*: Graph with initial data from the characteristic function with 1023 grid points using the coefficient $\alpha^2$ with a final time of $10^{-0}$

| $\alpha^3$, *Sin2x* | | | | | | |
|---|---|---|---|---|---|---|
| | | EigExp | | C-N | `ode15s` | |
| $t_f$ | $N$ | time | terms | time | time | $\Delta t_{\text{avg}}$ |
| 0.01 | 1023 | 0.036 | 75 | 0.006 | 0.025 | 3.846e-04 |
| | 2047 | 0.024 | 75 | 0.008 | 0.039 | 4.000e-04 |
| | 4095 | 0.021 | 75 | 0.018 | 0.078 | 3.846e-04 |
| 0.1 | 1023 | 0.008 | 24 | 0.006 | 0.030 | 2.381e-03 |
| | 2047 | 0.006 | 24 | 0.010 | 0.052 | 2.326e-03 |
| | 4095 | 0.010 | 24 | 0.019 | 0.129 | 2.174e-03 |
| 1 | 1023 | 0.006 | 9 | 0.006 | 0.057 | 1.163e-02 |
| | 2047 | 0.008 | 9 | 0.011 | 0.099 | 1.190e-02 |
| | 4095 | 0.010 | 9 | 0.022 | 0.289 | 1.099e-02 |

*Table 4.5*:

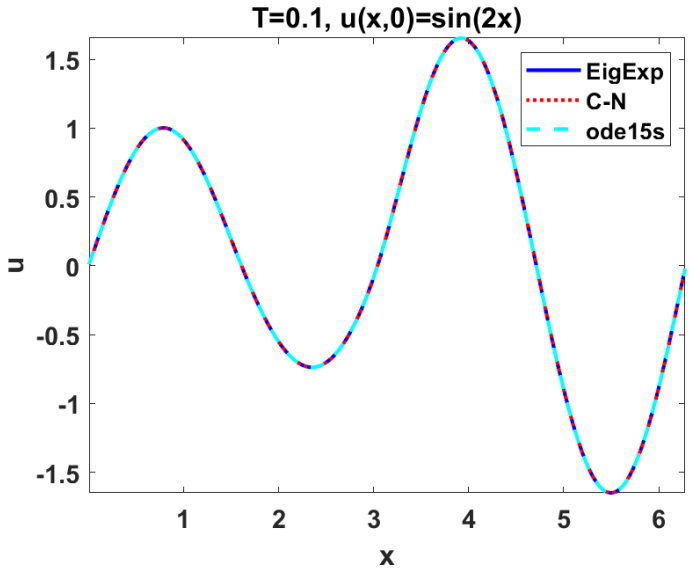


*Figure 4.9*: Graph with initial data *sin*2*x* with 1023 grid points using the coefficient $\alpha^3$ with a final time of $10^{-1}$

| $\alpha^3$, CharFunc | | | | | | |
|---|---|---|---|---|---|---|
| | | EigExp | | C-N | `ode15s` | |
| $t_f$ | $N$ | time | terms | time | time | $\Delta t_{\text{avg}}$ |
| 0.01 | 1023 | 0.018 | 75 | 0.006 | 0.069 | 1.053e-04 |
| | 2047 | 0.026 | 75 | 0.011 | 0.137 | 8.929e-05 |
| | 4095 | 0.036 | 75 | 0.018 | 0.321 | 7.692e-05 |
| 0.1 | 1023 | 0.006 | 24 | 0.005 | 0.073 | 8.065e-04 |
| | 2047 | 0.009 | 24 | 0.011 | 0.178 | 7.042e-04 |
| | 4095 | 0.021 | 24 | 0.027 | 0.389 | 6.289e-04 |
| 1 | 1023 | 0.010 | 9 | 0.010 | 0.179 | 6.135e-03 |
| | 2047 | 0.006 | 9 | 0.012 | 0.164 | 5.525e-03 |
| | 4095 | 0.009 | 9 | 0.024 | 0.392 | 5.051e-03 |

*Table 4.6*:

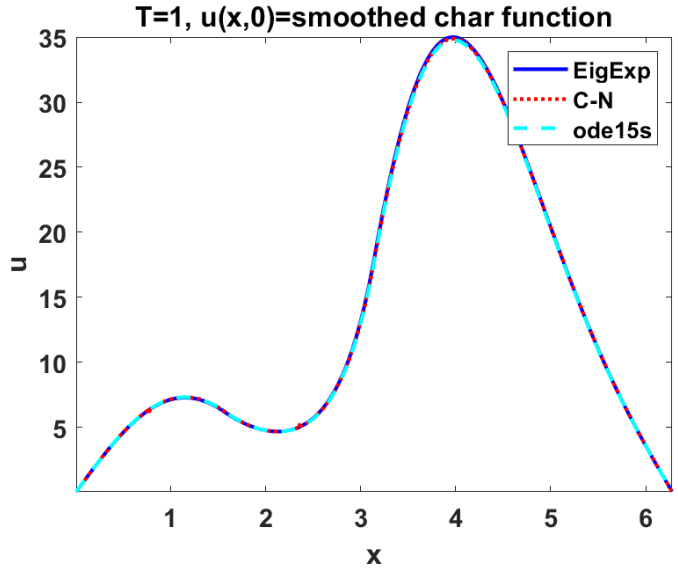


*Figure 4.10*: Graph with initial data from the characteristic function with 1023 grid points using the coefficient $\alpha^3$ with a final time of $10^{-0}$

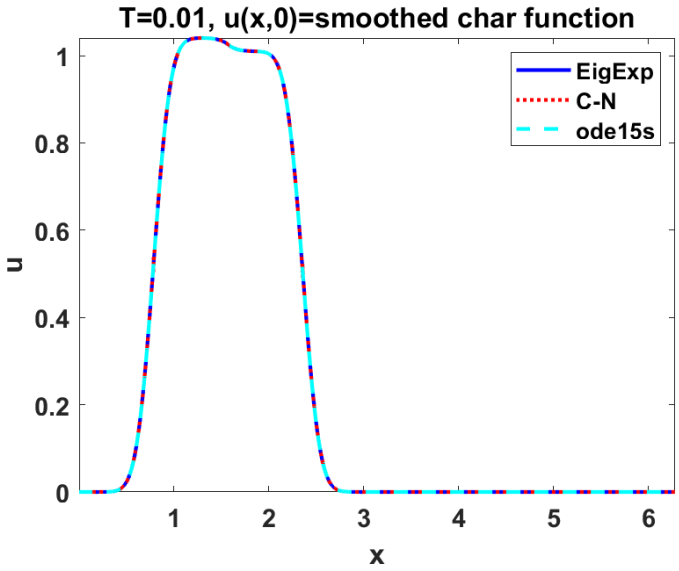


*Figure 4.11*: Graph with initial data from the characteristic function with 4095 grid points using the coefficient $\alpha^3$ with a final time of $10^{-2}$

| $\alpha^1$, $Sin2x$ | | | | | | |
|---|---|---|---|---|---|---|
| | | EigExp | | C-N | `ode15s` | |
| $t_f$ | $N$ | error | terms | error | error | $\Delta t_{\text{avg}}$ |
| 0.01 | 1023 | 1.8e-05 | 75 | 1.7e-04 | 1.5e-04 | 7.692e-04 |
| | 2047 | 1.9e-05 | 75 | 5.7e-05 | 1.2e-04 | 7.143e-04 |
| | 4095 | 1.9e-05 | 75 | 5.6e-05 | 1.1e-04 | 6.667e-04 |
| 0.1 | 1023 | 5.7e-05 | 24 | 5.2e-04 | 5.2e-04 | 3.226e-03 |
| | 2047 | 5.7e-05 | 24 | 1.7e-04 | 1.7e-04 | 3.226e-03 |
| | 4095 | 5.7e-05 | 24 | 1.7e-04 | 1.7e-04 | 3.030e-03 |
| 1 | 1023 | 1.1e-04 | 9 | 2.5e-03 | 1.1e-03 | 1.818e-02 |
| | 2047 | 1.1e-04 | 9 | 1.4e-03 | 1.5e-03 | 1.786e-02 |
| | 4095 | 1.1e-04 | 9 | 5.5e-04 | 5.0e-04 | 1.724e-02 |

*Table 4.7*:

| $\alpha^1$, CharFunc | | | | | | |
|---|---|---|---|---|---|---|
| | | EigExp | | C-N | `ode15s` | |
| $t_f$ | $N$ | error | terms | error | error | $\Delta t_{\text{avg}}$ |
| 0.01 | 1023 | 7.6e-03 | 75 | 7.9e-03 | 7.9e-03 | 1.053e-04 |
| | 2047 | 3.2e-03 | 75 | 3.4e-03 | 3.4e-03 | 8.929e-05 |
| | 4095 | 1.1e-03 | 75 | 1.6e-02 | 1.1e-03 | 7.692e-05 |
| 0.1 | 1023 | 2.6e-03 | 24 | 6.6e-03 | 3.6e-03 | 8.065e-04 |
| | 2047 | 1.1e-03 | 24 | 8.7e-02 | 1.5e-03 | 7.042e-04 |
| | 4095 | 3.8e-04 | 24 | 2.5e-01 | 5.6e-04 | 6.289e-04 |
| 1 | 1023 | 2.6e-03 | 9 | 2.3e-01 | 5.0e-02 | 6.536e-03 |
| | 2047 | 1.2e-03 | 9 | 3.4e-01 | 1.2e-02 | 5.848e-03 |
| | 4095 | 4.8e-04 | 9 | 4.2e-01 | 1.1e-02 | 5.319e-03 |

*Table 4.8*:

| $\alpha^2$, $Sin2x$ | | | | | | |
|---|---|---|---|---|---|---|
| | | EigExp | | C-N | `ode15s` | |
| $t_f$ | $N$ | error | terms | error | error | $\Delta t_{\text{avg}}$ |
| 0.01 | 1023 | 2.0e-07 | 75 | 2.2e-06 | 2.0e-06 | 4.348e-04 |
| | 2047 | 2.0e-07 | 75 | 6.4e-07 | 4.5e-07 | 4.348e-04 |
| | 4095 | 2.0e-07 | 75 | 1.7e-07 | 4.1e-07 | 4.167e-04 |
| 0.1 | 1023 | 2.1e-05 | 24 | 2.4e-04 | 2.4e-04 | 2.564e-03 |
| | 2047 | 2.1e-05 | 24 | 1.1e-04 | 1.1e-04 | 2.439e-03 |
| | 4095 | 2.1e-05 | 24 | 3.7e-05 | 4.1e-05 | 2.326e-03 |
| 1 | 1023 | 6.6e-04 | 9 | 3.0e+00 | 2.4e+00 | 1.408e-02 |
| | 2047 | 6.6e-04 | 9 | 1.9e+00 | 1.2e+00 | 1.370e-02 |
| | 4095 | 6.6e-04 | 9 | 1.3e+00 | 6.8e-01 | 1.351e-02 |

*Table 4.9*:

| $\alpha^2$, CharFunc | | | | | | |
|---|---|---|---|---|---|---|
| | | EigExp | | C-N | `ode15s` | |
| $t_f$ | $N$ | error | terms | error | error | $\Delta t_{\text{avg}}$ |
| 0.01 | 1023 | 7.6e-03 | 75 | 7.9e-03 | 7.9e-03 | 1.053e-04 |
| | 2047 | 3.2e-03 | 75 | 3.4e-03 | 3.4e-03 | 8.929e-05 |
| | 4095 | 1.1e-03 | 75 | 1.6e-02 | 1.1e-03 | 7.692e-05 |
| 0.1 | 1023 | 2.9e-03 | 24 | 6.5e-03 | 3.5e-03 | 8.000e-04 |
| | 2047 | 1.2e-03 | 24 | 8.7e-02 | 1.5e-03 | 7.042e-04 |
| | 4095 | 4.2e-04 | 24 | 2.5e-01 | 5.0e-04 | 6.250e-04 |
| 1 | 1023 | 3.8e-03 | 9 | 2.1e-01 | 4.5e-02 | 6.211e-03 |
| | 2047 | 1.8e-03 | 9 | 3.4e-01 | 2.0e-02 | 5.618e-03 |
| | 4095 | 8.8e-04 | 9 | 4.2e-01 | 8.2e-03 | 5.102e-03 |

*Table 4.10*:

| $\alpha^3$, $Sin2x$ | | | | | | |
|---|---|---|---|---|---|---|
| | | EigExp | | C-N | `ode15s` | |
| $t_f$ | $N$ | error | terms | error | error | $\Delta t_{\text{avg}}$ |
| 0.01 | 1023 | 6.6e-07 | 75 | 8.7e-06 | 8.5e-06 | 3.846e-04 |
| | 2047 | 6.6e-07 | 75 | 2.9e-06 | 2.5e-06 | 4.000e-04 |
| | 4095 | 6.6e-07 | 75 | 8.5e-07 | 4.9e-07 | 3.846e-04 |
| 0.1 | 1023 | 4.8e-05 | 24 | 5.7e-04 | 5.6e-04 | 2.381e-03 |
| | 2047 | 4.8e-05 | 24 | 2.4e-04 | 2.3e-04 | 2.326e-03 |
| | 4095 | 4.8e-05 | 24 | 7.9e-05 | 7.5e-05 | 2.174e-03 |
| 1 | 1023 | 7.5e-04 | 9 | 1.8e+00 | 2.5e+00 | 1.163e-02 |
| | 2047 | 7.5e-04 | 9 | 7.9e-01 | 1.0e+00 | 1.190e-02 |
| | 4095 | 7.5e-04 | 9 | 1.3e+00 | 3.1e-01 | 1.099e-02 |

*Table 4.11*:

| $\alpha^3$, CharFunc | | | | | | |
|---|---|---|---|---|---|---|
| | | EigExp | | C-N | `ode15s` | |
| $t_f$ | $N$ | error | terms | error | error | $\Delta t_{\text{avg}}$ |
| 0.01 | 1023 | 7.6e-03 | 75 | 7.9e-03 | 7.9e-03 | 1.053e-04 |
| | 2047 | 3.2e-03 | 75 | 3.4e-03 | 3.4e-03 | 8.929e-05 |
| | 4095 | 1.1e-03 | 75 | 1.6e-02 | 1.1e-03 | 7.692e-05 |
| 0.1 | 1023 | 2.9e-03 | 24 | 6.7e-03 | 3.7e-03 | 8.065e-04 |
| | 2047 | 1.2e-03 | 24 | 8.7e-02 | 1.6e-03 | 7.042e-04 |
| | 4095 | 4.0e-04 | 24 | 2.5e-01 | 5.2e-04 | 6.289e-04 |
| 1 | 1023 | 7.9e-03 | 9 | 2.3e-01 | 8.7e-02 | 6.135e-03 |
| | 2047 | 3.9e-03 | 9 | 3.5e-01 | 4.7e-02 | 5.525e-03 |
| | 4095 | 1.9e-03 | 9 | 4.2e-01 | 3.2e-02 | 5.051e-03 |

*Table 4.12*:

# Chapter 5

# Conclusion

The goal of this project was to develop an algorithm to efficiently solve the parabolic equation with a piecewise constant coefficient. This would allow us to better model sound acoustics in the ocean where the sound speed changes as the depth within the ocean increases. Our approach was to compute the eigenfunction expansion of the solution and find natural frequencies where the sound speed changes. When looking at the eigenvalues of this operator, we saw that the eigenvalues were a mixture of positive and negative values. Because of the varied positive and negative eigenvalues, this created many interesting challenges. We found that the function $\sin(\frac{jx}{2})$ was a good approximation of the eigenfunctions associated with the negative eigenvalues; however, the positive eigenvalues had to be found differently. The positive eigenvalues correspond to eigenfunctions that can be approximated by a linear combination of $\sin(\frac{jx}{2})$. In order to find this combination, we computed $A_0$ which is the restriction in the basis of the subspace $\Phi_J$ and solved for its eigenvalues. These eigenvalues were then used to find the initial guesses for the Secant Method. The Secant Method was used to find the exact eigenvalues for each piece, and then the eigenfunctions can be constructed from those. The method of eigenfunction expansion is a more accurate and efficient method of solving this problem. We were able to test our method using various parameters and it was efficient in low and high resolutions, with varying values for $\alpha$, and using different initial data. This method proved to work in cases that Crank-Nicolson did not, and it scaled much better than the ODE solver that Matlab uses.

In the future, this method could be improved by including a method that would handle complex $\omega$ values. This would mean that instead of using the trigonometric formulas for the eigenfunction expansion, we would convert this to the exponential case and use this as the eigenfunction

$$V_j(x) = \begin{cases} A_1 e^{\omega_1 x} + B_1 e^{-\omega_1 x} & 0 \le x < 2\pi\rho_1 \\ A_2 e^{\omega_2 x} + B_2 e^{-\omega_2 x} & 2\pi\rho_1 \le x < 2\pi\rho_2 \\ A_3 e^{\omega_3 x} + B_3 e^{-\omega_3 x} & 2\pi\rho_2 \le x < 2\pi \end{cases}$$

Another variation of this project could include a more accurate sound speed. In this project, we took the average of the sound speed since it was nearly constant and then bounded that with two constants to creat our piecewise constant coefficient. We would like to see if there is a method to transform the true sound speed operator to our piecewise constant operator in

order to solve the problem with the true sound speed instead of the average sound speed. This project could also be expanded to generalize to two dimensions. The original problem used cylindrical coordinates, so the additional variable would be $\theta$.

# BIBLIOGRAPHY


[1] Arfken, G. B., Weber, H. J. and Harris, F. (2012) *Mathematical Methods for Physicists: A Comprehensive Guide*, 7th Edition. Waltham, MA: Academic Press.

[2] Ascher, Uri M. and Greif, Chen (2011) *A First Course in Numerical Methods*, Vancouver, British Colombia: SIAM.

[3] Axler, Sheldon (1997) *Linear Algebra Done Right*, 2nd Edition. New York, NY: Springer.

[4] Burden, R. L. and Faires, J. D. (2010) *Numerical Analysis*, 9th Edition. Stamford, CT: Cengage Learning.

[5] Farlow, S. J. (1993) *Partial Differential Equations for Scientists and Engineers*. New York, NY: Dover Publications, Inc.

[6] Fefferman, C. (1983) The Uncertainty Principle. *Bulletin of the American Mathematical Society* **9**, 129-206.

[7] E. M. Garon and J. V. Lambers, "Modeling the Diffusion of Heat Energy within Composites of Homogeneous Materials using the Uncertainty Principle", *Computational and Applied Mathematics*, in review.

[8] B. Gustafsson, H.-O. Kreiss, and J. Oliger, *Time-Dependent Problems and Difference Methods*, Wiley, New York, 1995.

[9] K.E. Gilbert, M.J. White, "Application of the parabolic equation", *The Journal of the Acoustical Society of America* **85**(1989), p. 630-637.

[10] Harville, D. A. (1997). *Matrix Algebra From a Statistician's Perspective*. Springer-Verlag.

[11] J. V. Lambers, "Approximate Diagonalization of Variable-Coefficient Differential Operators Through Similarity Transformations", *Computers and Mathematics with Applications* **64**(8) (2012), p. 2575-2593.

[12] S. D. Long, S. Sheikholeslami, J. V. Lambers and C. Walker, "Diagonalization of 1-D Differential Operators with Piecewise Constant Coefficients Using the Uncertainty Principle", *Mathematics and Computers in Simulation* **156** (2019), p. 194-226.

[13] M. S. Min and D. Gottlieb, "On the Convergence of the Fourier Approximation for Eigenvalues and Eigenfunctions of Discontinuous Problems", *SIAM J. Numer. Anal.* **40**(6) (2003), p. 2254-2269.

[14] Simon, Barry (1985) The Theory of Schrödinger Operators: What's It All About? *Engineering and Science*, **48**(5). pp. 20-25.